Targeting the Cyclin E-Cdk-2 Complex Represses Lung Cancer Growth by Triggering Anaphase Catastrophe

Fabrizio Galimberti[1], Sarah L. Thompson[2], Xi Liu[1], Hua Li[1], Vincent Memoli[3,5], Simon R. Green[7], James DiRenzo[1,5], Patricia Greninger[6], Sreenath V. Sharma[6], Jeff Settleman[6], Duane A. Compton[2,5], and Ethan Dmitrovsky[1,4,5]

Abstract

Purpose: Cyclin-dependent kinases (Cdk) and their associated cyclins are targets for lung cancer therapy and chemoprevention given their frequent deregulation in lung carcinogenesis. This study uncovered previously unrecognized consequences of targeting the cyclin E–Cdk-2 complex in lung cancer.

Experimental Design: Cyclin E, Cdk-1, and Cdk-2 were individually targeted for repression with siRNAs in lung cancer cell lines. Cdk-2 was also pharmacologically inhibited with the reversible kinase inhibitor seliciclib. Potential reversibility of seliciclib effects was assessed in washout experiments. Findings were extended to a large panel of cancer cell lines using a robotic-based platform. Consequences of cyclin E–Cdk-2 inhibition on chromosome stability and on *in vivo* tumorigenicity were explored as were effects of combining seliciclib with different taxanes in lung cancer cell lines.

Results: Targeting the cyclin E–Cdk-2 complex, but not Cdk-1, resulted in marked growth inhibition through the induction of multipolar anaphases triggering apoptosis. Treatment with the Cdk-2 kinase inhibitor seliciclib reduced lung cancer formation in a murine syngeneic lung cancer model and decreased immunohistochemical detection of the proliferation markers Ki-67 and cyclin D1 in lung dysplasia spontaneously arising in a transgenic cyclin E–driven mouse model. Combining seliciclib with a taxane resulted in augmented growth inhibition and apoptosis in lung cancer cells. Pharmacogenomic analysis revealed that lung cancer cell lines with mutant ras were especially sensitive to seliciclib.

Conclusions: Induction of multipolar anaphases leading to anaphase catastrophe is a previously unrecognized mechanism engaged by targeting the cyclin E–Cdk-2 complex. This exerts substantial antineoplastic effects in the lung. *Clin Cancer Res; 16(1); 109–20. ©2010 AACR.*

Cyclin-dependent kinases (Cdk) are key regulators of cell cycle progression (1–3). Cdk-2 and its partner, cyclin E, regulate the G_1 to S cell cycle transition by phosphorylating the retinoblastoma protein (4). Engineered cyclin E overexpression shortens the cell cycle and causes chromosomal instability (5, 6). Aberrant cyclin E expression is frequently found in pulmonary dysplasia and lung cancer (7). This predicts an unfavorable clinical prognosis in lung cancer (8). Evidence for a critical role for the cyclin E–Cdk-2 complex in lung carcinogenesis came from prior work

showing that tobacco-carcinogen exposure deregulated cyclin E–Cdk-2 expression (9). That cyclin E–Cdk-2 was a therapeutic or chemopreventive target was independently shown following treatment with agents that induced proteasomal degradation of cyclin E or Cdk-2 (9–11).

Direct support for the importance of cyclin E in lung carcinogenesis came from engineered mouse models where human surfactant C–targeted expression of wild-type or proteasome degradation–resistant cyclin E species recapitulated many features of human lung carcinogenesis, including onset of chromosomal instability, hedgehog pathway deregulation, presence of premalignant and malignant lung lesions, and even metastases (12). These findings set the stage for the current study, which genetically repressed cyclin E expression with different small interfering RNAs (siRNA) and by pharmacologically inhibiting Cdk-2 activity with a small molecule kinase inhibitor, seliciclib (CYC202, R-roscovitine).

Seliciclib is a 2,6,9-trisubstituted purine analogue. It is an orally bioavailable inhibitor of Cdk activity that reversibly competes for binding to the ATP pocket of the kinase catalytic subunit (13, 14). Seliciclib prominently inhibits Cdk-2, but affects Cdk-1, Cdk-7, and Cdk-9 much less (15–17). Antitumor activity is reported against many human

Authors' Affiliations: Departments of [1]Pharmacology and Toxicology, [2]Biochemistry, [3]Pathology, [4]Medicine, and [5]Norris Cotton Cancer Center, Dartmouth Medical School, Hanover, New Hampshire and Dartmouth-Hitchcock Medical Center, Lebanon, New Hampshire; [6]Center for Molecular Therapeutics, Massachusetts General Hospital Cancer Center, Charlestown, Massachusetts; and [7]Cyclacel Ltd., Dundee, United Kingdom

Translational Relevance

Cyclins and cyclin-dependent kinases (Cdk) are important antineoplastic targets in oncology. Genetic and pharmacologic targeting of the cyclin E–Cdk-2 complex each resulted in marked growth inhibition of lung cancer cells through a previously unrecognized mechanism: induction of multipolar anaphases leading to apoptosis. Pharmacologic targeting of Cdk-2 with seliciclib reduced lung cancer formation *in vivo*. Treatments also decreased expressed proliferation markers in lung carcinogenesis lesions arising in transgenic cyclin E mice. Pharmacogenomic analysis revealed that lung cancer cell lines that exhibited marked sensitivity to seliciclib frequently harbored activating ras mutations. Cooperative antineoplastic effects were seen when seliciclib was combined with a microtubule-targeting agent such as a taxane. Together, these findings provide a strong rationale for combining a microtubule-targeting agent with Cdk-2 inhibition for lung cancer therapy, especially when ras mutations are present.

cancer cell lines, including those of breast, prostate, and lung cancer origins (16). A seliciclib phase I clinical trial is reported (14) and phase II trials are ongoing in non–small cell lung cancer (NSCLC) and nasopharyngeal carcinoma (18).

Consequences of targeting the cyclin E–Cdk-2 complex in human and murine lung cancer cell lines were explored in this study. This was accomplished by genetic knockdown of cyclin E with different siRNAs and by pharmacologic inhibition of Cdk-2 with seliciclib. Comparisons were made to effects observed following targeting of Cdk-1. Novel murine lung cancer cell lines derived from wild-type (ED-1) and proteasome degradation–resistant (ED-2) cyclin E–driven lung cancers (19) were studied as was a well-characterized panel of human lung cancer cell lines. Unexpectedly, seliciclib antineoplastic effects were only partially reversed after its washout. This provided a basis for pursuit of an involved mechanism.

Seliciclib was found to induce aberrant multipolar anaphases leading to anaphase catastrophe and apoptosis in lung cancer cells. This provided a mechanistic explanation for the antineoplastic effects of targeting Cdk-2. Combining seliciclib with different microtubule-targeting agents (paclitaxel or docetaxel) was used to search for agents that cooperate with seliciclib to augment anaphase catastrophe. A high-throughput cancer cell line platform was used to determine the extent and incidence of seliciclib-mediated growth suppression in diverse cancer cells. To establish therapeutic relevance of these findings, *in vivo* antineoplastic effects of inhibiting Cdk-2 were explored after murine lung cancer cells were injected through the tail veins of syngeneic FVB mice. Antineoplastic effects of seliciclib were also studied in transgenic cyclin E mice that spontaneously developed lung dysplasia or cancer (12).

Findings reveal prominent induction of anaphase catastrophe in lung cancer cells. This represents a previously unrecognized consequence of Cdk-2 inhibition. Taken together, these studies uncover a novel mechanism engaged by targeting the cyclin E–Cdk-2 complex that not only causes anaphase catastrophe, but also leads to apoptosis and significant repression of lung cancer growth *in vivo*. The implications of these findings for lung cancer therapy and potentially for chemoprevention will be discussed.

Materials and Methods

Chemicals and antibodies. Seliciclib (CYC202, R-roscovitine) was provided by Cyclacel Ltd, and 10 mmol/L stock solutions in DMSO were prepared and stored at −20°C until used. Docetaxel (Cytoskeleton) and paclitaxel (LC Laboratories) were each purchased. DMSO 10 mmol/L stock solutions were prepared for each agent and stored at −20°C. Fetal bovine serum (Gemini Bioproducts, Inc.) was purchased. Anti–cyclin D1 (product sc-718), anti-actin (product sc-1615), and horseradish peroxidase–conjugated donkey anti-goat IgG (product sc-2020) antibodies were purchased (Santa Cruz Biotechnology, Inc.) as were anti–COOH terminus domain RNA Polymerase II phosphorylated Ser-2 antibodies (Covance), the ECL Plus immunoblotting detection reagent (GE Healthcare UK Limited), and Protease Arrest protease inhibitor mixture (Geno Technology, Inc.).

Immunoblot analyses. Cells were lysed with ice-cold radioimmunoprecipitation lysis buffer, and immunoblot analyses were done, as described (20). Thirty-five micrograms of protein were loaded onto each lane. Lysates were size fractionated by SDS-PAGE before transfer to nitrocellulose membranes (Schleicher and Schuell Bioscience) and probing with the indicated antibodies.

Cell culture. Murine lung cancer cell lines were each derived from transgenic mice (12) harboring lung cancers expressing human surfactant C–driven wild-type cyclin E (ED-1 cell line) or proteasome degradation–resistant cyclin E (ED-2 cell line) species, as previously described (19). ED-1 and ED-2 murine lung cancer lines as well as C-10 murine immortalized lung epithelial cells and human lung cancer cell lines (HOP-62, H-522, and H-23) were each cultured in RPMI 1640 supplemented with 10% fetal bovine serum and 1% antibiotic and antimycotic solution at 37°C in 5% CO_2 in a humidified incubator.

Transient transfection. Logarithmically growing ED-1 (3×10^4) and ED-2 (4×10^4) cells were individually plated onto each well of a six-well tissue culture plate 24 h before transfection. The transfection procedures were done with Oligofectamine reagent (Invitrogen) and siRNAs targeting both murine and human cyclin E species as well as for Risc control siRNA (Dharmacon). Two different siRNAs were engineered that targeted both human and murine cyclin E coding sequences, as follows: 5′-AAGTGCTACTGCCGCAGTATC-3′ (siRNA-E1.1) and 5′-CCTCCAAAGTTGCACCAGTTT-3′

(siRNA-E1.2). Two different siRNAs were also engineered that targeted the Cdk-2 coding sequence, as follows: 5′-TTGCGATAACAAGCTCCG-3′ (Cdk-2.1) and 5′-TAAG-TACGAACAGGGACTC-3′ (Cdk-2.2). Two different siRNAs were engineered that targeted the Cdk-1 coding sequence, as follows: 5′-TCAAAGATGAGATATAAC-3′ (Cdk-1.1) and 5′-TTTGGATGATGACGAAGTTCC-3′ (Cdk-1.2). Fresh medium was added to each well 24 h after transfection. Three replicate experiments were done and each experiment was conducted in at least triplicates.

Real-time reverse transcription-PCR assays. Total RNA was isolated from the indicated siRNA-transfected ED-1 or ED-2 cells using Trizol reagent (Invitrogen). Reverse transcription (RT) assays were done using the High Capacity cDNA Reverse Transcription kit (Applied Biosystems) with a Peltier Thermal Cycler (MJ Research). Quantitative real-time PCR assays were done using SYBR Green PCR Mastermix (Applied Biosystems) and the 7500 Fast Real-time PCR System (Applied Biosystems) for quantitative detection of mRNAs. Reverse transcription-PCR assays were conducted using previously optimized protocols of the vendor (Applied Biosystems). Three replicate experiments were done. The primers used were as follows: murine cyclin E forward, 5′-GTGGCTCCGACCTTTCAGTC-3′ and reverse, 5′-CACAGTCTTGTCAATCTTGGCA-3′; murine Cdk-2 forward, 5′-CCTGCTTATCAATGCAGAGGG-3′ and reverse: 5′-TGCGGGTCACCATTTCAGC-3′; and murine glyceraldehyde-3-phosphate dehydrogenase forward: 5′-AGGTCGGTGTGAACGGATTTG-3′, and reverse: 5′-TGTAGACCATGTAGTTGAGGTCA-3′.

Proliferation and apoptosis assays. ED-1 (4.5×10^3), ED-2 (7.5×10^3), C-10 (8×10^3), H-23 (2×10^4), HOP-62 (4.5×10^3), and H-522 (2×10^4) cells were each seeded per well of a six-well tissue culture plate and treated 24 h later with the indicated agents. At least three wells were seeded for each cell line in each experiment. Triplicate replicate experiments were done. Logarithmically growing cells were assayed using the CellTiter-Glo assay (Promega) and established methods (21). Trypan blue viability assays were done, as described (21). Cellular apoptosis was measured by Annexin V:FITC positivity detected by flow cytometry using the Annexin V assay kit (AbD Serotec), following the vendor's methods.

Clonal growth assays. Two hundred logarithmically growing ED-1 cells were plated onto each 10-cm tissue culture plate. Triplicate replicate clonal growth assays were done. Cell cultures were treated with the indicated agent on day 1. Media were removed on day 4, and plates were incubated for an additional 10 d in seliciclib-free medium; otherwise, colonies did not readily form (data not shown). Colonies were stained with Diff Quick (IMEB, Inc.) according to the vendor's recommended procedures. Colonies were counted using the Oxford Optronix Col Count colony counter (Oxford Optronix) as in prior work (22).

Washout assays. ED-1 (1.5×10^4) and ED-2 (3×10^4) cells were each seeded onto 10-cm tissue culture plates and treated 24 h later with seliciclib (10 μmol/L) or vehicle (DMSO). Cells were washed thrice with sterile PBS

before being harvested and seeded in six-well plates, as described above. Seliciclib or vehicle (DMSO) were added 12 h later. Proliferation was monitored 48 and 96 h following treatments using the CellTiter-Glo assay (Promega).

Chromosome stability assay. ED-1, ED-2, C-10, H-23, HOP-62, and H-522 cells were each fixed in 3.5% paraformaldehyde, stained with anti-α-tubulin–specific antibody (Sigma Aldrich) and independently mounted with Pro-Long Gold antifade reagent supplemented with 4′,6-diamidino-2-phenylindole (Invitrogen). Stained cells were examined using an Eclipse TE 2000-E microscope (Nikon). Anaphase cells that contained three or more spindle poles were scored as multipolar.

High-throughput proliferation assay. In brief, 270 human cancer cell lines were seeded in 96-well microtiter plates (BD Biosciences), with each cell line seeded onto 3 different wells, as previously described (23, 24). These cells were treated with 0.15, 1.5, and 15 μmol/L seliciclib dosages. Cells were assayed 72 h posttreatment by staining with the fluorescent nucleic acid stain Syto 60 (Molecular Probes) using the Sciclone ALH300 multichannel liquid handling workstation (Caliper Lifesciences) and optimized methods (23, 24). Quantification of the fluorescent signals was done with the SpectraMax M5 plate reader (Molecular Devices). Means of triplicate seliciclib treatment experiments were compared with vehicle-treated cells, using optimized methods previously reported (23, 24).

In vivo seliciclib pharmacodynamic studies. Three 9-mo-old female mice expressing transgenic wild-type human cyclin E were each injected i.p. twice daily for 5 consecutive d with 100 mg/kg seliciclib or vehicle (DMSO), for a total of six mice in this experiment. These mice were then sacrificed following an Institutional Animal Care and Use Committee–approved protocol, and harvested lung tissues were formalin fixed, paraffin embedded, and sectioned for histopathologic analyses using previously established techniques (19). In addition to H&E staining, immunohistochemical staining for Ki-67 and cyclin D1 expression was detected using optimized techniques (12). Histopatholgic analyses were done by a pathologist (V. M.), who was unaware whether tissues harvested from mice were previously treated with seliciclib or with the vehicle.

In vivo tumorigenicity. Early passages of ED-1 cells were harvested in PBS supplemented with 10% mouse serum (Invitrogen) and 8×10^5 cells were individually injected into the tail veins of each of 8-wk-old female FVB mice. Ten mice were each i.p. treated twice daily, 5 d on, 2 d off, for 3 cycles with 100 mg/kg seliciclib, and 10 additional mice were treated with vehicle (DMSO). Treatments began 2 wk after tail vein injections. This time was selected because ED-1 cells had already begun to form lung tumors at this time point (data not shown). A replicate experiment was done. Mice were then sacrificed following an Institutional Animal Care and Use Committee–approved protocol, and harvested lung tissues were formalin fixed, paraffin embedded, and sectioned for histopathologic analyses using established methods (19, 25). Analyses

were done by a pathologist (H. L.) who was unaware of which mice were treated with seliciclib or vehicle.

Statistical analysis. All assays were expressed as means ± SD. Results of all independent experiments were pooled to assess for statistical significance. *Z* test and two-sided *t* tests were used for all statistical analyses. Statistical significance was considered for values of $P < 0.05$ and $P < 0.01$, respectively.

Results

Targeting cyclin E expression. To investigate effects of knockdown of cyclin E independently in ED-1 and ED-2 murine lung cancer cells, two siRNAs were designed to target both endogenous murine and exogenous human cyclin E species. Findings were compared with an inactive control siRNA. Over 95% of cells were transiently transfected with the desired siRNAs (data not shown). To validate knockdown of targeted mRNAs, real-time quantitative reverse transcription-PCR assays were done using total RNA isolated from transfected ED-1 or ED-2 cells. Marked knockdown of cyclin E mRNAs was achieved in both ED-1 and ED-2 cells, as shown in Fig. 1A. The result

was that both ED-1 and ED-2 cellular proliferation was markedly inhibited, as in Fig. 1B. This inhibition was consistent with a likely dependence on cyclin E expression for both ED-1 and ED-2 cell growth. When higher siRNA dosages targeting cyclin E were used in transfection experiments, few viable cells remained (data not shown).

Inhibition of Cdk-2. To confirm and extend evidence for importance of the cyclin E–Cdk-2 complex in lung cancer cell growth, Cdk-2 was pharmacologically targeted with seliciclib, a reversible Cdk-2 inhibitor. Cdk-2 inhibition caused a significant dose-dependent growth suppression of both ED-1 and ED-2 cells at 48 and 96 hours, compared with vehicle controls occurring at seliciclib dosages of 10 to 25 μmol/L (Fig. 2A). Seliciclib treatment decreased clonal growth in a dose-dependent manner (Fig. 2B). Seliciclib treatment also led to a substantial repression of cyclin D1 protein expression by 48 hours, but inhibited phosphorylation of RNA-polymerase II at Ser-2, a hallmark of Cdk-7/9 inhibition (16), only at high dosages (25 μmol/L; Fig. 2C). Thus, the biological effects of seliciclib at dosages below 25 μmol/L were due to Cdk-2 inhibition rather than to repression of transcription through Cdk-7/9 blockade.
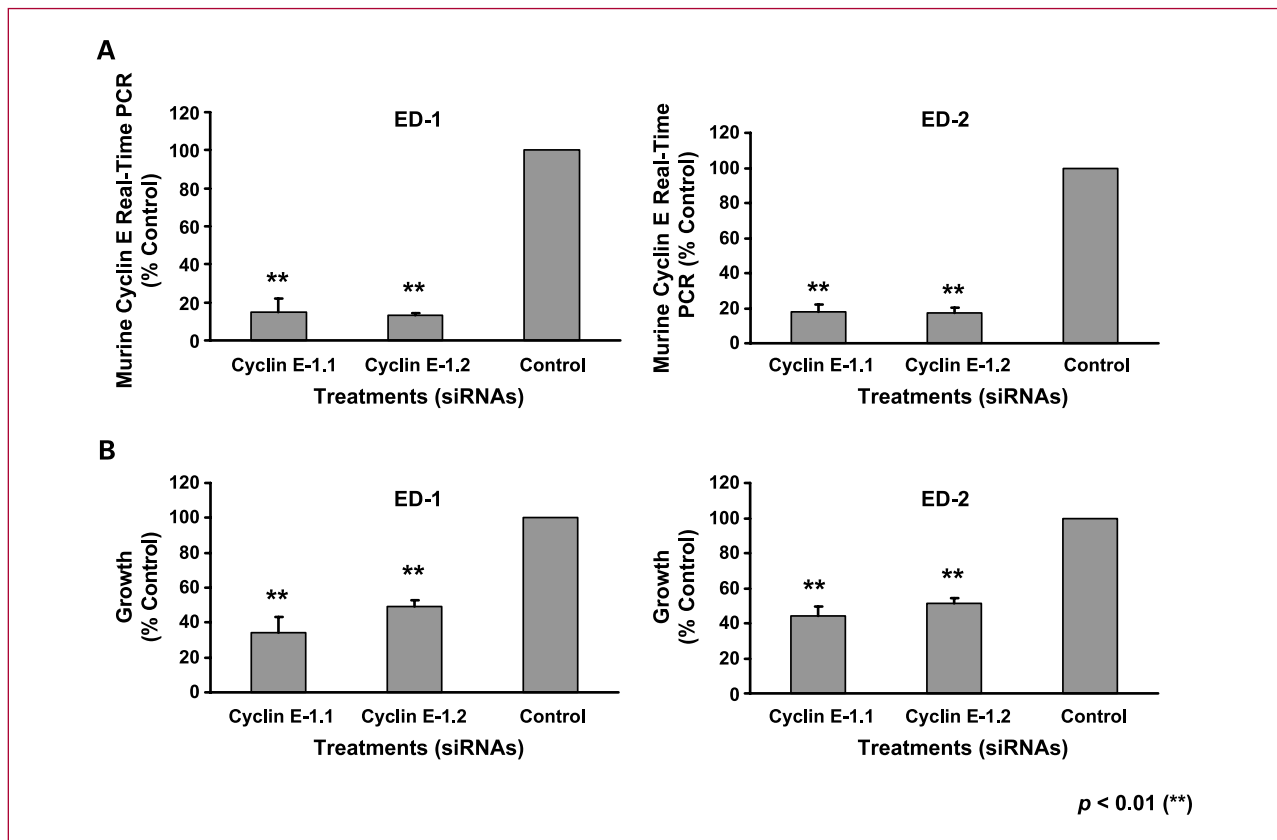

Fig. 1. Individual siRNA-mediated knockdown of cyclin E species repressed growth of ED-1 and ED-2 lung cancer cell lines. *A,* confirmation of cyclin E mRNA knockdown by real-time reverse transcription-PCR assays performed on RNA isolated from ED-1 (*left*) and ED-2 (*right*) cells transfected with different siRNAs targeting both human and murine cyclin E species or with RISC-free siRNA (*control*). *B,* proliferation of ED-1 (*left*) and ED-2 (*right*) cells was inhibited by these siRNAs targeting cyclin E. Columns, mean; bars, SD.
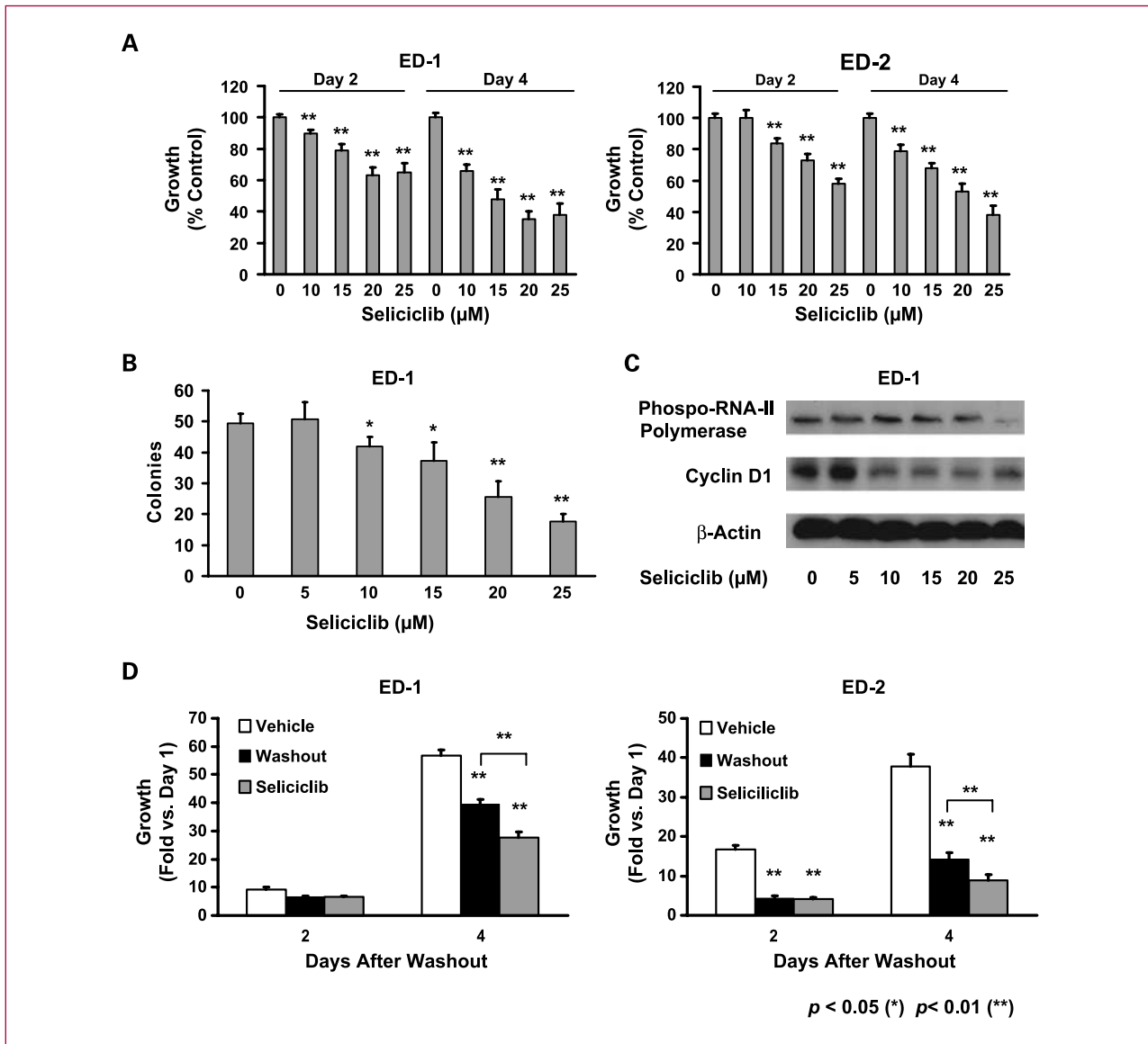
Fig. 2. Cdk-2 inhibition repressed proliferation and clonal growth of ED-1 and ED-2 lung cancer cells. *A*, dose- and time-dependent inhibition of ED-1 (*left*) and ED-2 (*right*) cell growth by seliciclib compared with vehicle (DMSO) control. *B*, seliciclib treatment reduced clonal growth of ED-1 cells in a dose-dependent manner. *C*, dose-dependent effects of pharmacologic inhibition of Cdk-2 with seliciclib resulted in downregulation of cyclin D1 protein by immunoblot analysis of ED-1 cells. RNA-polymerase II phosphorylation was inhibited by seliciclib treatment only at a dosage of 25 μmol/L (a dosage above those examined for antineoplastic effects). Actin expression served as a loading control. *D*, seliciclib effects were partially reversed in ED-1 (*left*) and ED-2 (*right*) cells as seen in washout experiments at the 10 μmol/L dosage, as shown in this figure. ED-1 and ED-2 cell growth only partially recovered from seliciclib washout compared with cells continuously treated with seliciclib. SD bars and *P* values are displayed.

Intriguingly, seliciclib-mediated growth inhibition was only partially reversed by washout experiments conducted in ED-1 and ED-2 cells (Fig. 2D). This was the basis for pursuit of an engaged mechanism from targeting Cdk-2. Given the known induction of chromosomal instability by cyclin E overexpression (6), effects of Cdk-2 inhibition on chromosome stability of ED-1, ED-2, and other lung cancer cells were explored. Seliciclib treatment increased the occurrence of multipolar anaphases, which has been shown to result in cell death (Fig. 3A and B, *left*; ref. 26).

This mechanism associated with seliciclib therapeutic effects occurred in both ED-1 and ED-2 cells.

To investigate whether inhibition of Cdk-2 was responsible for induction of multipolar anaphases, Cdk-2 was sublethally targeted with two different siRNAs. Notably, Cdk-2 knockdown resulted in marked growth inhibition, which was consistent with a likely addiction of ED-1 and ED-2 cells to cyclin E and its partner, Cdk-2, for their growth. Quantitative PCR (Supplementary Fig. S1A) was done after sublethal knockdown of Cdk-2 through

different siRNAs. This resulted in induction of apoptosis (Supplementary Fig. S1B) and increased multipolar anaphases (Fig. 3B, right), whereas comparable siRNA-mediated Cdk-1 knockdown (Supplementary Fig. S1B) did not result in a significant increase in apoptosis or multipolar anaphases (Fig. 3B, right). Thus, specifically targeting Cdk-2 resulted in multipolar anaphases leading to anaphase catastrophe.

Cdk-2 inhibition by seliciclib resulted in growth inhibition of HOP-62, H-522, and H-23 human lung cancer cell lines (Supplementary Fig. S2A). Seliciclib treatment also augmented multipolar anaphases leading to anaphase catastrophe in each of these human lung cancer cell lines as early as 4 hours after seliciclib (15 μmol/L) treatment (Fig. 3C-D). In contrast, C-10–immortalized murine pulmonary epithelial cells had much less basal aneuploidy than lung cancer cells and exhibited only minor growth inhibition after seliciclib treatment (Supplementary Fig. S2B). This treatment (15 μmol/L of seliciclib) did not significantly induce multipolar anaphases in C-10 cells (Fig. 3D, right). Thus, both human and murine lung cancer cell lines exhibited statistically significant growth inhibition and induction of anaphase catastrophe after seliciclib treatments. These findings, along with results from a large panel of cancer cell lines (discussed below), revealed that antiproliferative effects of inhibiting Cdk-2 are frequent in lung cancer cells as well as in many other cancer cell lines.

Seliciclib cooperation with taxanes. Taxanes are microtubule-targeting agents that confer apoptosis through mechanisms that include induction of mitotic catastrophe (27). Given this, studies of the consequences of combining seliciclib with these agents were undertaken. Paclitaxel and docetaxel were the taxanes (27, 28) examined. Combining seliciclib with either paclitaxel or docetaxel caused at least additive growth inhibition of ED-1 (Fig. 4A) and ED-2 lung cancer cells (data not shown). Each agent was used at dosages lower than used in single agent studies to search for cooperative interactions. These treatment regimens cooperatively increased induction of apoptosis (Fig. 4B) and reduced clonal growth (Fig. 4C). Notably, combined treatment of seliciclib with paclitaxel or docetaxel led to at least additive growth inhibition of HOP-62, H-522, and H-23 human lung cancer cell lines compared with vehicle controls (Supplementary Fig. S2C). Thus, dual targeting of Cdk-2 with seliciclib and microtubules with either paclitaxel or docetaxel exerted cooperative antiproliferative effects in murine and human lung cancer cell lines.

High-throughput studies. To comprehensively examine seliciclib effects, a recently described method for detecting pharmacologic responses was used with a large number of cancer cell lines and a robotic-based platform (23, 24). A total of 270 human cancer cell lines from diverse cancer histopathologic types was investigated. Over half of investigated lung, pancreatic, head and neck, esophageal, liver, thyroid, ovarian, uterine, and skin cancer cell lines showed at least 50% growth inhibition following 72 hours of

seliciclib treatment, compared with vehicle treated cells (Supplementary Table S1; Fig. 5A). Among the 270 human cancer cell lines investigated, 52 were of NSCLC origin and 2 (4%) were relatively insensitive to seliciclib (fractional growth, >75% compared with vehicle-treated cells), whereas 21 (40%) displayed a modest sensitivity (fractional growth was between 75% and 50% compared with vehicle-treated cells), and 29 (56%) showed marked sensitivity scored as fractional growth <50% versus controls (Fig. 5B).

Effects of seliciclib treatments on proliferation of H-522 lung cancer cells were also investigated in Supplementary Fig. S2A with concordant results as in this high-throughput experiment. As shown, this cell line was less sensitive than others examined and had wild-type ras status (Supplementary Table S2). The ras status of 13 of 15 NSCLC cell lines with highest sensitivity to seliciclib is known.[8] Intriguingly, analyses revealed that 12 of 13 (92%) of the lung cancer cells most sensitive to seliciclib treatments had K-ras– or N-ras–activating mutations, whereas none of the NSCLC cell lines with the least sensitivity to seliciclib had such mutations (Supplementary Table S2; Fig. 5C). Prior work has shown that both H-23 and HOP-62 lung cancer cells harbor ras mutations and, as shown in Supplementary Table S1, are more sensitive to seliciclib than H-522 lung cancer cells (29). Thus, findings from this large panel of cancer cell lines indicated significant seliciclib sensitivity well beyond those human and murine lung cancer cells already investigated. For lung cancer cells, this response is tightly associated with the presence of ras activation in highly responsive cells.

Seliciclib effects in transgenic cyclin E mice. To investigate seliciclib pharmacodynamic effects in the lungs of transgenic wild-type cyclin E mice that spontaneously develop lung carcinogenesis, seliciclib 100 mg/kg or vehicle (DMSO) were each administered to mice i.p. twice a day, as described in the Materials and Methods. Immunohistochemical analyses revealed that seliciclib treatment resulted in a significantly decreased number of nuclei immunostaining for the pharmacodynamic markers Ki-67 ($P = 0.00011$) and cyclin D1 ($P = 0.00037$) in representative dysplastic lung lesions, compared with vehicle-treated control mice (Supplementary Fig. S3; Fig. 6A).

Seliciclib antineoplastic effects. ED-1 lung cancer cells (8×10^5) were tail vein injected into each syngeneic FVB mouse. These mice exhibited histopathologic evidence of lung adenocarcinomas by 2 weeks after injections of ED-1 cells (data not shown). Whether targeting Cdk-2 with seliciclib exerted antitumorigenic effects was examined in 10 female FVB mice per treatment arm after tail vein injections with ED-1 cells. Seliciclib treatment of each of these mice began 2 weeks following injection of cells. Results were compared with those obtained from 10 syngeneic female FVB vehicle-control–treated mice,
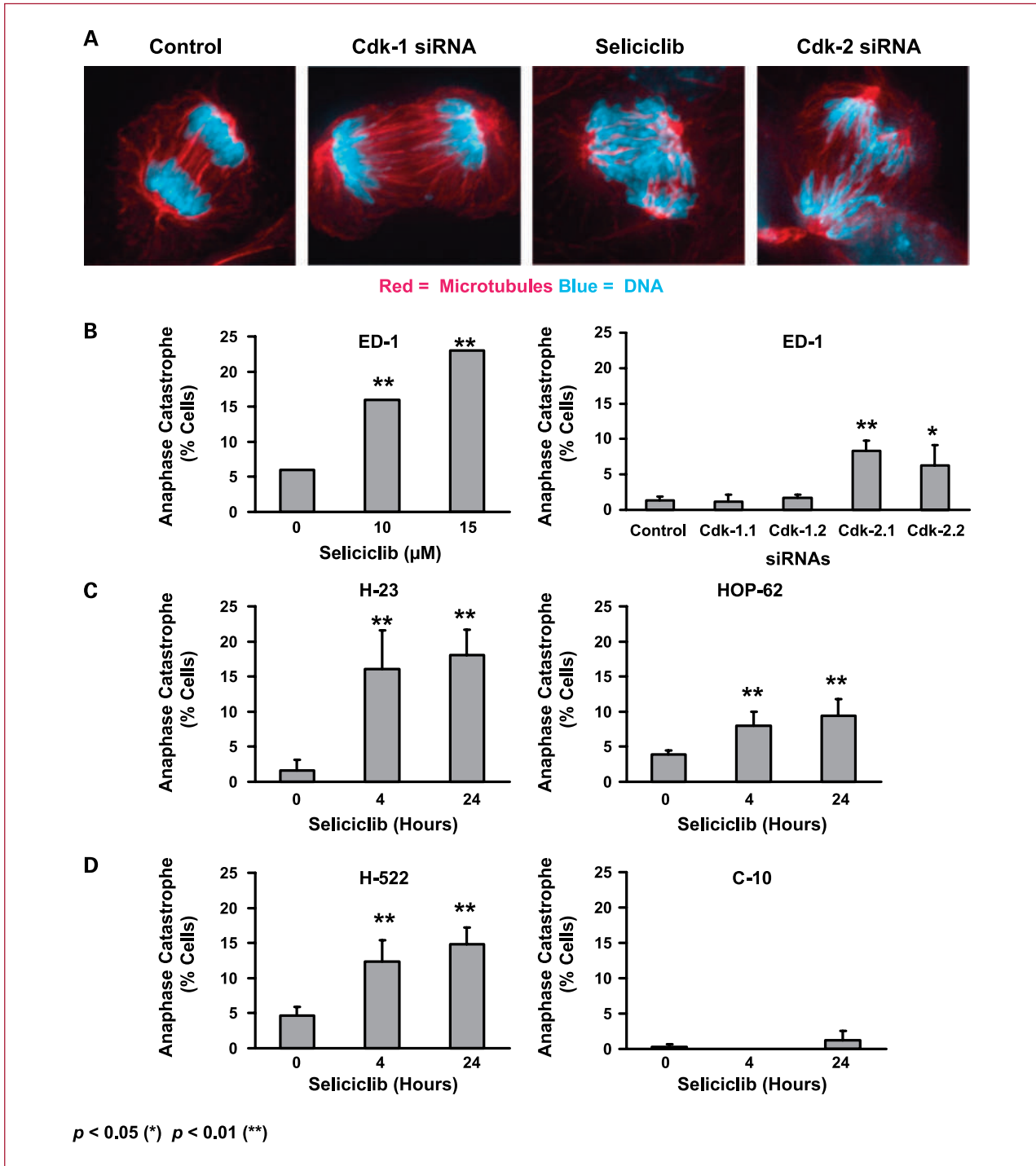

Fig. 3. Cdk-2 inhibition affects chromosomal stability by inducing multipolar anaphases in murine and human lung cancer cells, but not in C-10–immortalized murine lung epithelial cells. *A,* a representative ED-1 cell undergoing anaphase in the presence of control (vehicle, DMSO, or control siRNA) and two indepedendent Cdk-1 siRNAs (results from one representative siRNA experiment are shown), compared with another representative ED-1 cell undergoing multipolar anaphase in the presence of seliciclib (10 μmol/L) as well as following transfection of each of two different Cdk-2 siRNAs (results from one representative siRNA experiment are shown). ED-1 cells were fixed 24 h after treatment and stained, as described in the Materials and Methods. Microtubules were stained red and DNA was stained blue with 4′,6-diamidino-2-phenylindole. Cells in anaphase were scored for mulitpolar anaphases as in the Materials and Methods. *B, left,* a representative induction of multipolar anaphases in ED-1 cells 24 h after seliciclib treatments. *Right,* induction of anaphase catastrophe in ED-1 cells 24 h after transfection with each of two different Cdk-2 targeting siRNAs, two Cdk-1 siRNAs, and control siRNA. *C* and *D,* the percentage of H-23, HOP-62, and H-522 human lung cancer cells compared with C-10–immortalized murine pulmonary epithelial cells undergoing multipolar anaphases following seliciclib (15 μmol/L) treatment (*0 h,* control). SD bars and *P* values are shown.
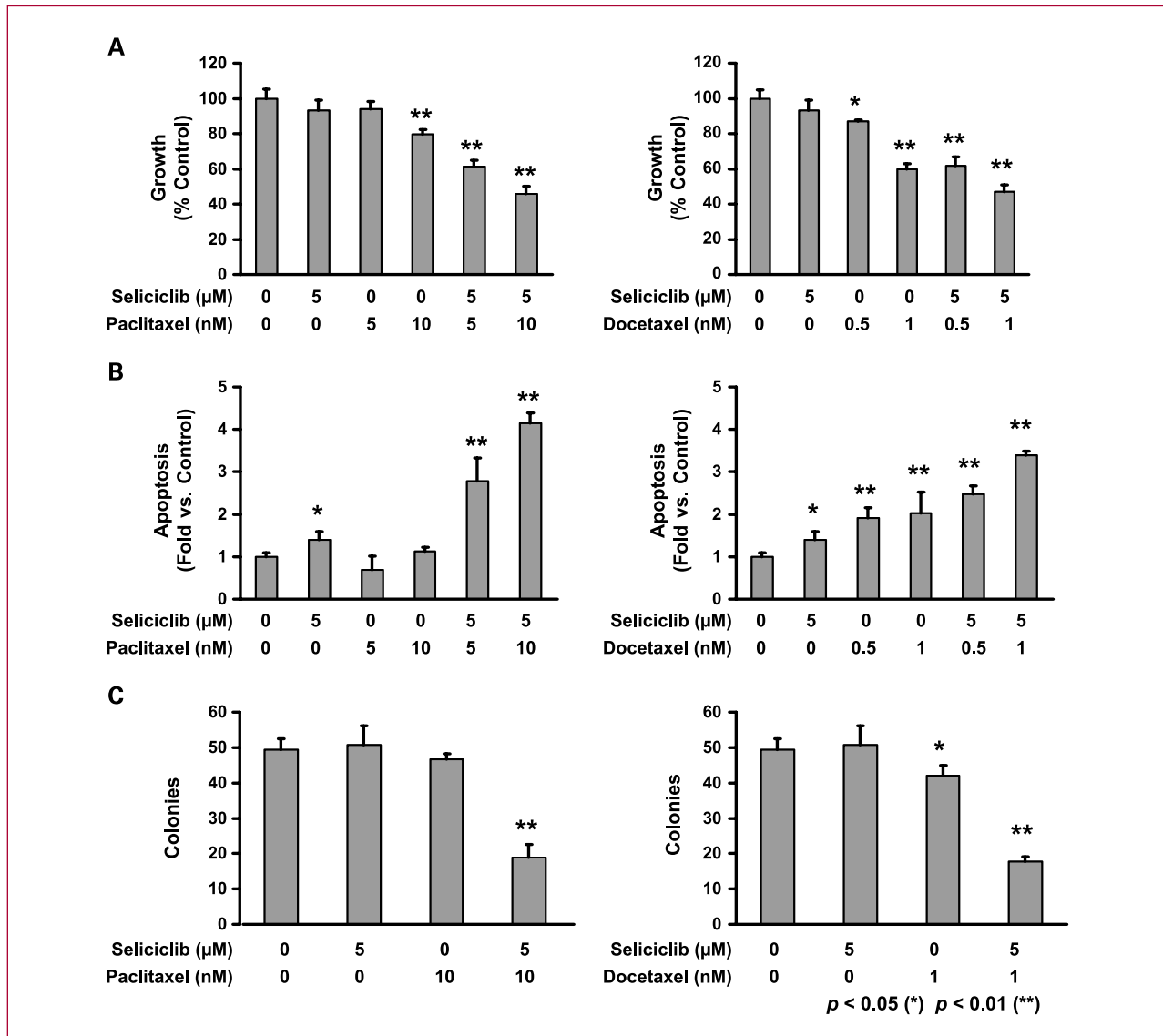
Fig. 4. Seliciclib and taxanes cooperatively inhibited proliferation and clonal growth, while inducing apoptosis of ED-1 lung cancer cells. *A,* seliciclib treatment combined with paclitaxel (*left*) or docetaxel (*right*) treatment cooperatively inhibited ED-1 cell growth compared with vehicle (DMSO) controls. *B,* seliciclib treatment combined with paclitaxel (*left*) or docetaxel (*right*) treatment increased apoptosis as detected by Annexin V:FITC and propidium iodide staining. *C,* cooperation between seliciclib and paclitaxel (*left*) or docetaxel (*right*) treatments significantly repressed ED-1 cell clonal growth. SD bars and *P* values are shown.

as described in the Materials and Methods. Numbers of lesions detected histopathologically in formalin-fixed paraffin-embedded lung tissue specimens were scored 6 weeks after ED-1 cell injections into FVB mice. Seliciclib treatment resulted in a significant reduction of high-grade ($P = 0.026$; Fig. 6C) and multilayer ($P = 0.005$; Fig. 6D) lung lesions, compared with the lungs of vehicle-treated FVB mice injected with ED-1 cells in each of two replicate experiments. Representative lesions are shown in Fig. 6B. The quantifications of lung lesions for one of the two replicate experiments are shown in Fig. 6C and D. Targeting Cdk-2 with seliciclib exerted significant antitumorigenic effects.

Discussion

Cyclin E and Cdk-2 are therapeutic targets deregulated in lung cancer (1–3). The current study advances prior work by showing that targeting the cyclin E–Cdk-2 complex triggers anaphase catastrophe and apoptosis that in turn substantially suppressed lung cancer growth. Recently described ED-1 and ED-2 murine transgenic lung cancer cells (19) depended on cyclin E expression for their growth, as confirmed by the marked growth inhibition resulting from siRNA-mediated knockdown of cyclin E (Fig. 1). The marked growth inhibitory effects observed in these cells likely indicated an addiction to cyclin E

(30). Cdk-2 inhibition with seliciclib decreased proliferation of ED-1 and ED-2 cells (Fig. 2A) as well as growth observed in a large panel of human cancer cells, including 52 lung cancer cell lines (Fig. 5A and B). This established the broad pharmacologic effect of targeting the cyclin E–Cdk-2 complex in cancer cells.

Unexpectedly, these effects were partially reversed (Fig. 2D). An intriguing engaged mechanism for this was found: induction of multipolar anaphases leading to anaphase catastrophe and apoptosis (Fig. 3). Apoptosis was enhanced by combining Cdk-2 inhibition with microtubule-targeting taxanes (Supplementary Fig. S2C; Fig. 4). Cdk-2 inhibition led to repression of pharmacodynamic proliferation markers and to reduced lung cancer formation *in vivo* (Fig. 6).

This has implications for translational cancer research. These findings underscore a clinical rationale for targeting the cyclin E–Cdk-2 complex in lung cancer patients.

Aberrant expression of cyclin E (6) and hCDC4 mutations (31) have each been previously reported to induce chromosomal instability. The known effects of cyclin E on chromosomal instability and aneuploidy were the basis for searching for their changing during cyclin E–Cdk-2 inhibition. Results presented in this study indicate that inhibition of Cdk-2 markedly affected chromosomal stability by inducing formation of multiple spindle poles triggering anaphase catastrophe. This underscored the critical role played by the cyclin E–Cdk-2 complex in the maintenance of chromosome stability. This effect was
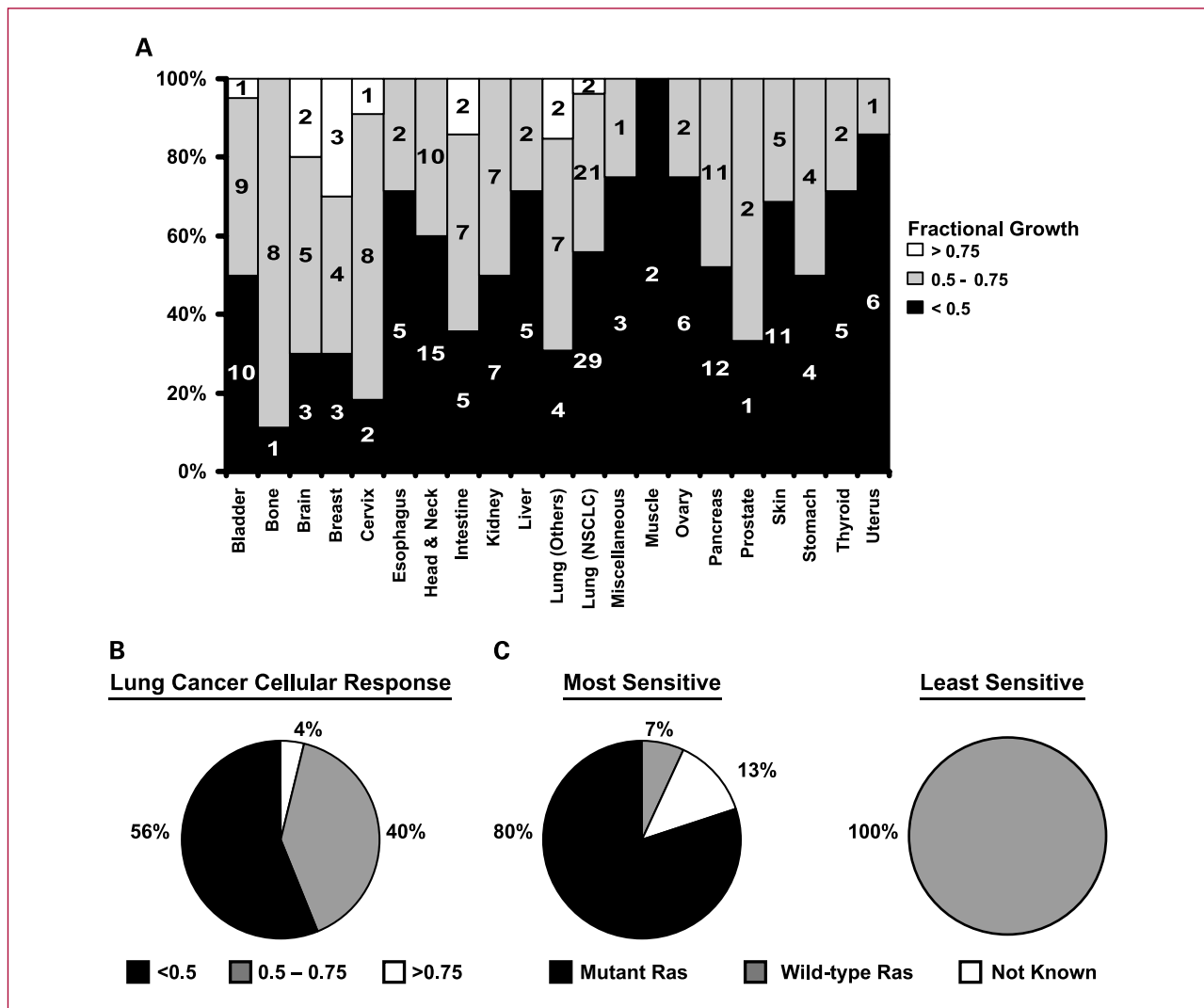

Fig. 5. Profiling for seliciclib sensitivity revealed growth inhibitory effects in diverse cancer cell lines. *A,* schematic representation of seliciclib sensitivity across 270 cancer cell lines from diverse tissues. *Lung (others),* four small-cell lung cancer, six mesothelioma, and one bronchial carcinoma cell lines. *Miscellaneous,* two fibrosarcoma, one fibrous histiocytoma, and one small round-cell sarcoma cancer cell lines. The complete set of data is presented in Supplementary Table S1. *B,* pie chart representation of NSCLC cell lines sensitivity to seliciclib (15 μmol/L) treatment. *C, left,* ras status for the 15 NSCLC cell lines with highest growth inhibitory response to seliciclib. *Right,* ras status for the 15 NSCLC cell lines with least growth inhibitory response to seliciclib.
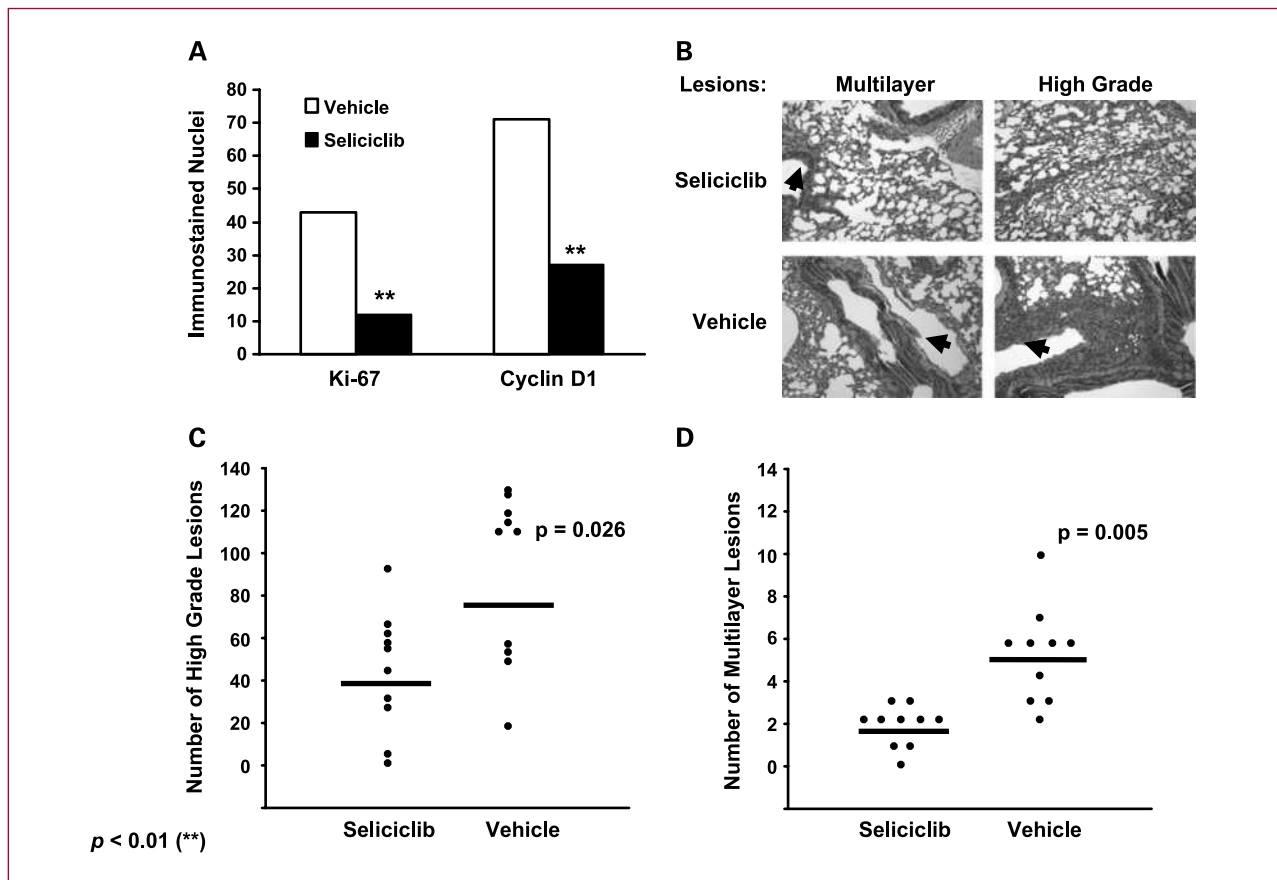
Fig. 6. *In vivo* seliciclib treatment effects. *A,* seliciclib treatment caused repression of Ki-67 and cyclin D1–immunostained nuclei in representative dysplastic lung lesions of wild-type cyclin E–expressing transgenic mice compared with vehicle-treated (DMSO) mice. *B,* representative H&E staining of lung tissues from syngeneic FVB mice injected with ED-1 lung cancer cells before *in vivo* treatment with seliciclib or vehicle (DMSO). *C,* seliciclib treatment resulted in reduced high-grade lesions (*P* = 0.026) in the lungs of ED-1 tail vein–injected syngeneic FVB mice compared with vehicle (DMSO) treatment. Each symbol represents a single mouse. *Line,* the mean number of high-grade lesions in each group. *D,* fewer multilayer lesions (*P* = 0.005) occurred in the lungs of ED-1 tail vein–injected syngeneic FVB mice treated *in vivo* with seliciclib compared with vehicle-treated (DMSO) mice. Each symbol represents a single mouse. *Line,* the mean number of multilayer lesions in each group.

observed at seliciclib dosages (≤20 μmol/L) that preferentially inhibited Cdk-2 activity and not RNA II polymerase, as shown in Fig. 2C. Targeting of Cdk-2 in ED-1 cells with siRNAs also led to induction of multipolar anaphases (Fig. 3B, *right*). Induction of multipolar anaphases was not observed following Cdk-1 knockdown (Fig. 3B, *right*), underscoring a specificity for Cdk-2 inhibition. Although a possible role for the cyclin B1-Cdk-1 complex in the induction of multipolar anaphases has been highlighted (32), Cdk-2 was shown in this study to play an important regulatory role especially when the cyclin E–Cdk-2 complex was active. Higher seliciclib dosages (Fig. 2A) as well as siRNAs engineered against cyclin E (Fig. 1) or Cdk-2 (data not shown) each led to marked cytotoxicity, as expected (30).

Future work will investigate the precise mechanism(s) leading to anaphase catastrophe. A possible Cdk-2 target is NuMA, a key organizer of mitotic spindle poles, and its activity is regulated by Cdks (33, 34). Comparing the phosphoproteome of seliciclib versus vehicle-treated lung cancer cells in future work should help elucidate the role of this target and perhaps identify others mediating these effects. Another target to consider is HSET, a kinesin motor that regulates the organization of centrosomes in dividing cells and is essential for cells undergoing division in the presence of extra centrosomes (26, 35).

Prior work and studies presented here indicate antitumorigenic effects of targeting the cyclin E–Cdk-2 complex in animal models and raise interest in targeting this pathway in diverse cancer cell contexts, including lung cancer (1, 16). Seliciclib as a single agent or as part of a combination regimen decreased tumor size in xenograft models (16, 17, 36). However, a phase I clinical trial with seliciclib as a single agent did not report objective responses (14).

Multiple reasons could account for this clinical observation. Prior proof of principle clinical trials by our team (37, 38) established that optimal intratumoral drug concentrations are needed to exert desired pharmacodynamic effects within clinical lung cancers. Clinical pharmacologic

data for seliciclib intratumoral concentrations in cancers of patients do not yet exist, but would provide critical information to guide the selection of an optimal seliciclib dose and schedule used in the treatment of cancer patients. It is also worth noting that seliciclib is a first-generation Cdk-2 inhibitor and newer compounds with greater potency are under study (39). Our preliminary studies reveal that several of these compounds are much more potent than seliciclib in conferring growth inhibition in lung cancer cells (data not shown). Furthermore, the use of pharmacodynamic markers identified in this study, such as the expression profile of cyclin E or presence of ras mutations within lung cancers might guide selection of lung cancer cases likely to be responsive to seliciclib.

Intriguingly, a tight correlation was found between ras mutations and sensitivity to seliciclib treatments in the high-throughput screen displayed in Fig. 5C and Supplementary Table S2. Activating ras mutations are found in a subset of NSCLCs (40) and this predicts resistance to epidermal growth factor receptor–tyrosine kinase inhibitors (41, 42). The presence of ras mutations was linked to chromosomal instability (43, 44), providing a plausible explanation for these mutations conferring sensitivity to seliciclib treatment through reduced chromosomal stability. This pharmacogenomic result indicated that cyclin E–Cdk-2 targeting therapies could be effective for lung cancer patients resistant to epidermal growth factor receptor–tyrosine kinase inhibitor–based therapy due to activating ras mutations.

Analyzing responses of patients from previous seliciclib clinical trials based on ras mutation status should provide clinical insights. Also, because combining seliciclib with microtubule-targeting agents produced cooperative antineoplastic effects in both murine (Fig. 4) and human (Supplementary Fig. S2C) lung cancer cells, a combination regimen of seliciclib with paclitaxel or docetaxel would be an attractive lung cancer therapeutic regimen to consider. Future work should not only explore cooperation between Cdk-inhibitors with taxanes, but also with other agents. In this regard, it is notable that preliminary studies indicate that seliciclib cooperates with all-*trans*-retinoic acid to suppress lung cancer cell growth (data not shown). Other combination regimens might be considered.

In summary, targeting the cyclin E–Cdk-2 complex led to significant suppression of lung cancer growth both *in vitro* and *in vivo.* Unexpectedly, a novel consequence of this inhibition was induction of anaphase catastrophe that triggered apoptosis. Kinase-targeted therapy has proven effective for targeting Bcr-Abl in chronic myelogenous leukemia (45, 46), c-kit in gastrointestinal stromal tumors (47), and epidermal growth factor receptor in lung cancer (48, 49). Prior work revealed a key role for the cyclin E–Cdk-2 complex in lung carcinogenesis (1, 12) and in lung cancer therapy or chemoprevention (1, 3, 9, 10, 12). This study advances prior work by implicating cyclin E–Cdk-2 complex inhibition, in combination with a microtubule-targeting agent, as a lung cancer therapeutic strategy.

Disclosure of Potential Conflicts of Interest

Grant Support

References

1. Shapiro GI. Cyclin-dependent kinase pathways as targets for cancer treatment. J Clin Oncol 2006;24:1770–83.

2. Koff A, Giordano A, Desai D, et al. Formation and activation of a cyclin E-cdk2 complex during the G1 phase of the human cell cycle. Science 1992;257:1689–94.

3. Freemantle SJ, Liu X, Feng Q, et al. Cyclin degradation for cancer therapy and chemoprevention. J Cell Biochem 2007;102: 869–77.

4. Harbour JW, Luo RX, Dei Santi A, Postigo AA, Dean DC. Cdk phosphorylation triggers sequential intramolecular interactions that progressively block Rb functions as cells move through G1. Cell 1999;98:859–69.

5. Ohtsubo M, Theodoras AM, Schumacher J, Roberts JM, Pagano M. Human cyclin E, a nuclear protein essential for the G1-to-S phase transition. Mol Cell Biol 1995;15:2612–24.

6. Spruck CH, Won KA, Reed SI. Deregulated cyclin E induces chromosome instability. Nature 1999;401:297–300.

7. Lonardo F, Rusch V, Langenfeld J, et al. Overexpression of cyclins D1 and E is frequent in bronchial preneoplasia and precedes squamous cell carcinoma development. Cancer Res 1999;59:2470–6.

8. Fukuse T, Hirata T, Naiki H, et al. Prognostic significance of cyclin E overexpression in resected non-small cell lung cancer. Cancer Res 2000;60:242–4.

9. Langenfeld J, Lonardo F, Kiyokawa H, et al. Inhibited transformation of immortalized human bronchial epithelial cells by retinoic acid is linked to cyclin E down-regulation. Oncogene 1996;13:1983–90.

10. Dragnev KH, Pitha-Rowe I, Ma Y, et al. Specific chemopreventive agents trigger proteasomal degradation of G1 cyclins: implications for combination therapy. Clin Cancer Res 2004;10:2570–7.

11. Sueoka N, Lee HY, Walsh GL, et al. Posttranslational mechanisms contribute to the suppression of specific cyclin:CDK complexes by all-trans retinoic acid in human bronchial epithelial cells. Cancer Res 1999;59:3838–44.

12. Ma Y, Fiering S, Black C, et al. Transgenic cyclin E triggers dysplasia

and multiple pulmonary adenocarcinomas. Proc Natl Acad Sci U S A 2007;104:4089–94.

13. De Azevedo WF, Leclerc S, Meijer L, et al. Inhibition of cyclin-dependent kinases by purine analogues: crystal structure of human cdk2 complexed with roscovitine. Eur J Biochem 1997;243:518–26.

14. Benson C, White J, De Bono J, et al. A phase I trial of the selective oral cyclin-dependent kinase inhibitor seliciclib (CYC202; R-Roscovitine), administered twice daily for 7 days every 21 days. Br J Cancer 2007;96:29–37.

15. Whittaker SR, Walton MI, Garrett MD, et al. The Cyclin-dependent kinase inhibitor CYC202 (R-roscovitine) inhibits retinoblastoma protein phosphorylation, causes loss of cyclin D1, and activates the mitogen-activated protein kinase pathway. Cancer Res 2004;64:262–72.

16. Fleming IN, Hogben M, Frame S, et al. Synergistic inhibition of ErbB signaling by combined treatment with seliciclib and ErbB-targeting agents. Clin Cancer Res 2008;14:4326–35.

17. McClue SJ, Blake D, Clarke R, et al. In vitro and in vivo antitumor properties of the cyclin dependent kinase inhibitor CYC202 (R-roscovitine). Int J Cancer 2002;102:463–8.

18. Guzi T. CYC-202 Cyclacel. Curr Opin Investig Drugs 2004;5:1311–8.

19. Liu X, Sempere LF, Galimberti F, et al. Uncovering growth-suppressive MicroRNAs in lung cancer. Clin Cancer Res 2009;15:1177–83.

20. Pitha-Rowe I, Hassel BA, Dmitrovsky E. Involvement of UBE1L in ISG15 conjugation during retinoid-induced differentiation of acute promyelocytic leukemia. J Biol Chem 2004;279:18178–87.

21. Petty WJ, Li N, Biddle A, et al. A novel retinoic acid receptor β isoform and retinoid resistance in lung carcinogenesis. J Natl Cancer Inst 2005;97:1645–51.

22. Feng Q, Sekula D, Guo Y, et al. UBE1L causes lung cancer growth suppression by targeting cyclin D1. Mol Cancer Ther 2008;7:3780–8.

23. McDermott U, Sharma SV, Dowell L, et al. Identification of genotype-correlated sensitivity to selective kinase inhibitors by using high-throughput tumor cell line profiling. Proc Natl Acad Sci U S A 2007;104:19936–41.

24. McDermott U, Sharma SV, Settleman J. High-throughput lung cancer cell line screening for genotype-correlated sensitivity to an EGFR kinase inhibitor. Methods Enzymol 2008;438:331–41.

25. Rusch V, Klimstra D, Venkatraman E, et al. Overexpression of the epidermal growth factor receptor and its ligand transforming growth factor α is frequent in resectable non-small cell lung cancer but does not predict tumor progression. Clin Cancer Res 1997;3:515–22.

26. Kwon M, Godinho SA, Chandhok NS, et al. Mechanisms to suppress multipolar divisions in cancer cells with extra centrosomes. Genes Dev 2008;22:2189–203.

27. McGrogan BT, Gilmartin B, Carney DN, et al. Taxanes, microtubules and chemoresistant breast cancer. Biochim Biophys Acta 2008;1785:96–132.

28. Eniu A, Palmieri FM, Perez EA. Weekly administration of docetaxel and paclitaxel in metastatic or advanced breast cancer. Oncologist 2005;10:665–85.

29. Koo HM, McWilliams MJ, Alvord WG, et al. Ras oncogene-induced sensitization to 1-β-D-arabinofuranosylcytosine. Cancer Res 1999;59:6057–62.

30. Weinstein IB, Joe A. Oncogene addiction. Cancer Res 2008;68:3077–80.

31. Rajagopalan H, Jallepalli PV, Rago C, et al. Inactivation of hCDC4 can cause chromosomal instability. Nature 2004;428:77–81.

32. Castedo M, Perfettini JL, Roumier T, et al. Cell death by mitotic catastrophe: a molecular definition. Oncogene 2004;23:2825–37.

33. Lydersen BK, Pettijohn DE. Human-specific nuclear protein that associates with the polar region of the mitotic apparatus: distribution in a human/hamster hybrid cell. Cell 1980;22:489–99.

34. Compton DA, Luo C. Mutation of the predicted p34cdc2 phosphorylation sites in NuMA impair the assembly of the mitotic spindle and block mitosis. J Cell Sci 1995;108:621–33.

35. Mountain V, Simerly C, Howard L, et al. The kinesin-related protein, HSET, opposes the activity of Eg5 and cross-links microtubules in the mammalian mitotic spindle. J Cell Biol 1999;147:351–66.

36. Tirado OM, Mateo-Lozano S, Notario V. Roscovitine is an effective inducer of apoptosis of Ewing's sarcoma family tumor cells in vitro and in vivo. Cancer Res 2005;65:9320–7.

37. Dragnev KH, Petty WJ, Shah SJ, et al. A proof-of-principle clinical trial of bexarotene in patients with non-small cell lung cancer. Clin Cancer Res 2007;13:1794–800.

38. Petty WJ, Dragnev KH, Memoli VA, et al. Epidermal growth factor receptor tyrosine kinase inhibition represses cyclin D1 in aerodigestive tract cancers. Clin Cancer Res 2004;10:7547–54.

39. Green SR, Frame S, Anderson S, et al. Derivatives of seliciclib with improved potency both in vitro and in vivo as novel cyclin dependent kinase (CDK) inhibitors [abstract]. Proceeding of the 100th Annual Meeting for Cancer Research. Philadelphia (PA): AACR; 2009, p. 3863.

40. Aviel-Ronen S, Blackhall FH, Shepherd FA, Tsao MS. K-ras mutations in non-small-cell lung carcinoma: a review. Clin Lung Cancer 2006;8:30–8.

41. Massarelli E, Varella-Garcia M, Tang X, et al. KRAS mutation is an important predictor of resistance to therapy with epidermal growth factor receptor tyrosine kinase inhibitors in non-small-cell lung cancer. Clin Cancer Res 2007;13:2890–6.

42. Eberhard DA, Johnson BE, Amler LC, et al. Mutations in the epidermal growth factor receptor and in KRAS are predictive and prognostic indicators in patients with non-small-cell lung cancer treated with chemotherapy alone and in combination with erlotinib. J Clin Oncol 2005;23:5900–9.

43. Castagnola P, Giaretti W. Mutant KRAS, chromosomal instability and prognosis in colorectal cancer. Biochim Biophys Acta 2005;1756:115–25.

44. Perera SA, Maser RS, Xia H, et al. Telomere dysfunction promotes genome instability and metastatic potential in a K-ras p53 mouse model of lung cancer. Carcinogenesis 2008;29:747–53.

45. Druker BJ, Tamura S, Buchdunger E, et al. Effects of a selective inhibitor of the Abl tyrosine kinase on the growth of Bcr-Abl positive cells. Nat Med 1996;2:561–6.

46. Druker BJ, Sawyers CL, Kantarjian H, et al. Activity of a specific inhibitor of the BCR-ABL tyrosine kinase in the blast crisis of chronic myeloid leukemia and acute lymphoblastic leukemia with the Philadelphia chromosome. N Engl J Med 2001;344:1038–42.

47. Sleijfer S, Wiemer E, Verweij J. Drug Insight: gastrointestinal stromal tumors (GIST)-the solid tumor model for cancer-specific treatment. Nat Clin Pract Oncol 2008;5:102–11.

48. Paez JG, Janne PA, Lee JC, et al. EGFR mutations in lung cancer: correlation with clinical response to gefitinib. Science 2004;304:1497–500.

49. Lynch TJ, Bell DW, Sordella R, et al. Activating mutations in the epidermal growth factor receptor underlying responsiveness of non-small cell lung cancer to gefitinib. N Engl J Med 2004;350:2129–39.